

Measurement of $D^0 \rightarrow \omega\eta$ Branching Fraction with CLEO-c Data

M. Smith

Lawrence Technological University

D. Cinabro

*Wayne State University, Department of Physics and Astronomy**

P. Naik

University of Bristol

(Dated: July 5, 2018)

Abstract

Using CLEO-c data, we confirm the observation of $D^0 \rightarrow \omega\eta$ by BESIII. In the Dalitz Plot of $D^0 \rightarrow K_s^0\eta\pi^0$, we find a background in the $K_s^0(\rightarrow \pi^+\pi^-)\pi^0$ projection with a $m(\pi^+\pi^-\pi^0)$ equal to the $\omega(782)$ mass. In a direct search for $D^0 \rightarrow \omega\eta$ we find a clear signal and measure $\mathcal{BF}_{D^0 \rightarrow \omega\eta} = (1.78 \pm 0.19 \pm 0.14) \times 10^{-3}$, in good agreement with BESIII.

* david.cinabro@wayne.edu

The recent observation by BESIII of $D^0 \rightarrow \omega\eta$ [1] gave clarity to us of a mystery we noted in CLEO-c data. In the Dalitz Plot of $D^0 \rightarrow K_s^0\eta\pi^0$, we observed an anomalous peak at 0.6 $(\text{GeV}/c^2)^2$ in the $m(K_s^0\pi^0)^2$ fit projection. The BESIII observation leads us to think that this peak is due to an $\omega(782) \rightarrow \pi^+\pi^-\pi^0$ candidate whose charged pions are mis-reconstructed as a K_s^0 . This decay channel has been predicted to have a $\mathcal{BF} = (3.3 \pm 0.2) \times 10^{-3}$ [2]. Charge conjugation is implied throughout. Since the decay can proceed from both a D^0 and a \bar{D}^0 and we do no additional reconstruction to find the D flavor, we are actually measuring the average of the branching fractions of $D^0 \rightarrow \omega\eta$ and $\bar{D}^0 \rightarrow \omega\eta$.

The CLEO-c detector and its experimental methods have been described in detail elsewhere [3]. This analysis was performed on 818 pb^{-1} of $e^+e^- \rightarrow \psi(3770)$ data with center-of-mass energy $E_{\text{cm}} = 3.774 \text{ GeV}$. All D^0/\bar{D}^0 candidates are reconstructed from π^\pm , π^0 , and η that pass standard selection criteria described elsewhere[4]. Charged tracks must be well reconstructed and pass basic track quality selections. We require a track momentum between $0.050 \text{ GeV}/c \leq p \leq 2 \text{ GeV}/c$ and the tracks consistent with coming from the interaction region. We use the specific ionization, dE/dx , from the drift chambers and the Ring Imaging CHerenkov (RICH) detector to identify our selected tracks as π^\pm . If dE/dx is valid, we require a three standard deviation consistency with the π^\pm hypothesis. For tracks with $p \geq 0.70 \text{ GeV}$ and $|\cos\theta| < 0.8$ we can use RICH information as well. If both RICH and dE/dx are valid, we require the combined log-likelihood $\mathcal{L}_{\pi K} \leq 0$ where

$$\mathcal{L}_{\pi K} = \sigma_\pi^2 - \sigma_K^2 + L_\pi - L_K \quad (1)$$

with L_h is the log-likelihood of the hypothesis from the RICH information.

We reconstruct π^0 and η candidates as neutral $\rightarrow \gamma\gamma$. The unconstrained mass is calculated under the assumption that the photons originate from the interaction point. We require this mass to be within 3σ of the nominal π^0/η mass. A subsequent kinematic fit must not be obviously bad, $\chi^2 < 10000$. We reject neutral candidates with both photons detected in the endcap of our calorimeter and explicitly reject any photon showers with a matched track. Aside from mass values the selections are identical for π^0 and η candidates.

We reconstruct D^0 candidates from $\pi^+\pi^-\pi^0\eta$ combinations. We make an initial requirement that the invariant mass $m(\pi^+\pi^-\pi^0\eta)$ be within $0.100 \text{ GeV}/c^2$ of the Particle Data Group PDG [5] average D^0 mass. We select $\omega(782)$ candidates with the $\pi^+\pi^-\pi^0$ invariant mass, m_ω . We choose selections on m_ω , the beam-constrained mass of $\omega\eta$ (M_{bc}), and

their ΔE in an iterative procedure making selections on two of the three, fitting a Gaussian signal plus smooth backgrounds in the third, making a selection based on the fit results, and repeating until the selection values do not change. In M_{bc} we fit the background to an Argus function, and use a 4th order polynomial in ΔE and m_ω . Unlike for M_{bc} there is no physics motivated background shape for ΔE and m_ω , and we chose the polynomial of high enough order to give a reasonable model of background without adding meaningless nuisance parameters. We use the signal mean and standard deviation from one fit to make three standard deviation selections on the other plots. We generate 50000 simulated signal D^0/\bar{D}^0 events to measure the efficiency of our reconstruction and to determine the optimal widths to use in fitting to the data. We take the yield from M_{bc} and ΔE as our measurements of the D^0 yield in the simulation. From the value of M_{bc} yield, we find an efficiency of $(17.49 \pm 0.216)\%$.

The same process is performed in data, but with the widths obtained in signal simulation fixed in fits to the data distributions. We choose $\omega(782)$ candidates which have $0.76016 \text{ GeV}/c^2 \leq m(\pi^+\pi^-\pi^0) \leq 0.80432 \text{ GeV}/c^2$. The $m(\pi^+\pi^-\pi^0)$ mass fit is used to select $\omega(782)$ candidates, but not for measurement of the D^0 yield. The ΔE , $E_{\pi^+\pi^-\pi^0\eta} - E_{Beam}$, distribution is shown in Figure 1. We set this selection to $-0.03525 \text{ GeV} \leq \Delta E \leq 0.03117 \text{ GeV}$. The beam-constrained mass, $M_{bc}^2 c^4 \equiv E_{Beam}^2 - p^2 c^2$, distribution and fit is shown in Figure 2, and we select $1.857675 \text{ GeV}/c^2 \leq M_{bc} \leq 1.871685 \text{ GeV}/c^2$. The M_{bc} and ΔE fit yields can both be used as measurements of the $D^0 \rightarrow \omega\eta$ yield. Raw signal yields are 711 ± 65 from the M_{bc} fit and 720 ± 70 from the ΔE fit. We show the $m(\pi^+\pi^-\pi^0)$ invariant mass distribution after the selections on M_{bc} and ΔE in Figure 3, noting that there is a clear ω signal.

Above, we assume the $\omega(782)$ is strongly related to the reconstruction of the D^0 and its M_{bc} . To better visualize this relation, we observe the two dimensional plot of $\omega(782)$ mass versus M_{bc} , subject to a three standard deviation ΔE cut. We clearly see a well-populated region near the intersection of the $D^0 M_{bc}$ and $\omega(782)$ mass rising above the large background. We also fit the M_{bc} distribution below and above the $\omega(782)$ selections. We find no clear D^0 signal presence in these sidebands.

We expect there to be some K_s^0 contamination in our $\omega(782)$ signal; after all we began with the opposite in $K_s^0\eta\pi^0$. For our signal candidates we show the $m(\pi^+\pi^-)$ distribution in Figure 4. There is a clear K_s^0 peak. This is fit using a Gaussian “signal” and 4th order

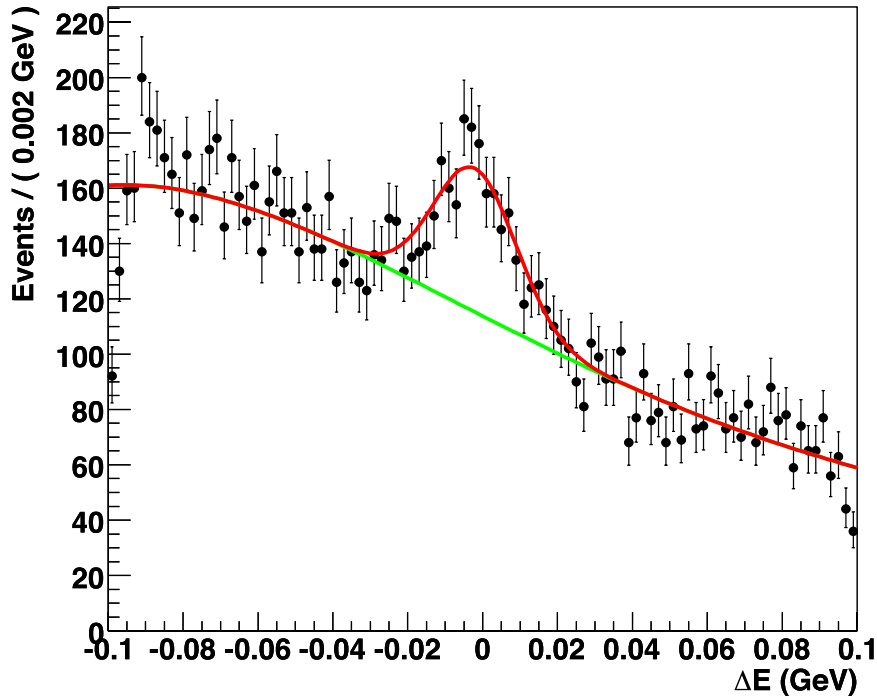


FIG. 1. The ΔE distribution and fit described in text after three standard deviation signal selections for the $\omega(782)$ and on M_{bc} .

polynomial “background” using the signal region selections above. We use this to estimate the K_s^0 background. We subtract the “signal” yield in Figure 4 from our previous results. We determine how many of the 158 ± 20 K_s^0 events should be subtracted by examining M_{bc} in three regions: three standard deviations around the K_s^0 mean and the two sidebands. We fit M_{bc} using the previously outlined method, and find the signal and background yields under the peak. Using the signal fraction in the K_s^0 region, we subtract 43 ± 17 from the observed yields. The K_s^0 subtraction value includes a 10% uncertainty due to our inability to precisely know how many K_s^0 are “signal” versus “background.”

In a second method of accounting for K_s^0 contamination we veto the $K_s^0\pi^0$ contribution to $\omega(782)$ by removing the K_s^0 region in $m(\pi^+\pi^-)$. Aside from the veto, the analysis is identical to that described above. We determine a new efficiency in fits to the veto M_{bc} distribution of $(16.13 \pm 0.208)\%$ which represents an 7.8% reduction with respect to the efficiency without the K_s^0 veto.

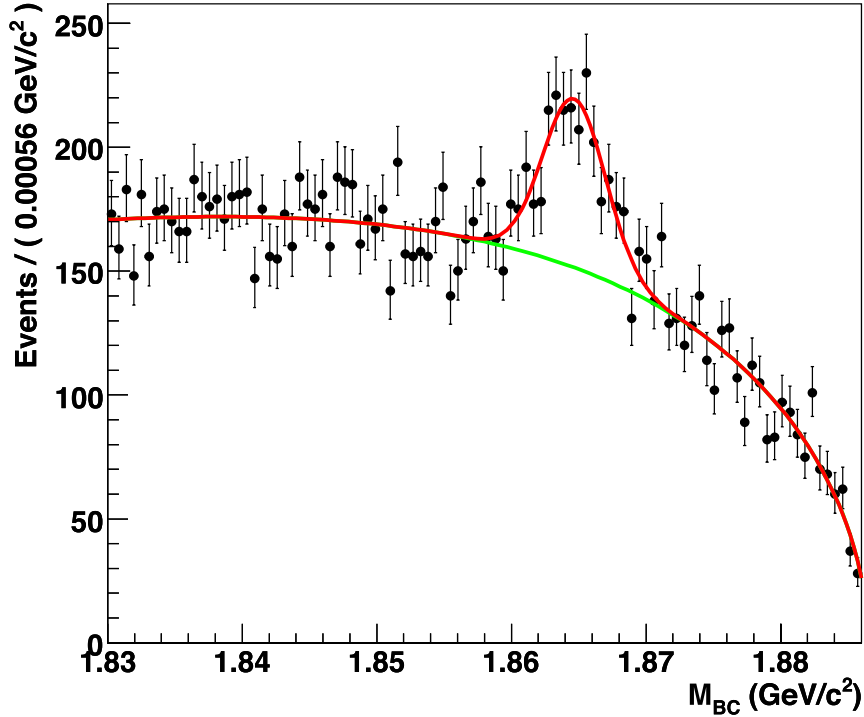


FIG. 2. The M_{bc} distribution and fit described in text after the three standard deviation signal selections on $\omega(782)$ and ΔE .

TABLE I. Signal and Background Yields From M_{bc} , Comparing Three $m(\pi^+\pi^-)$ Regions

$3\sigma M_{bc}$	In Relation to K_s^0 Peak		
	Below	In	Above
Signal	347	122	229
Background	1749	327	1649
Sig/Total	16.56%	27.17%	12.19%

Repeating the data analysis with the K_s^0 veto, Table II contains the K_s^0 veto analysis yields. Table III contains the yields from ΔE and M_{bc} corrected by both K_s^0 subtraction and veto, as well as their associated efficiencies and efficiency corrected yields.

The analyses described above used widths from Signal Monte Carlo fixed in the data fits.

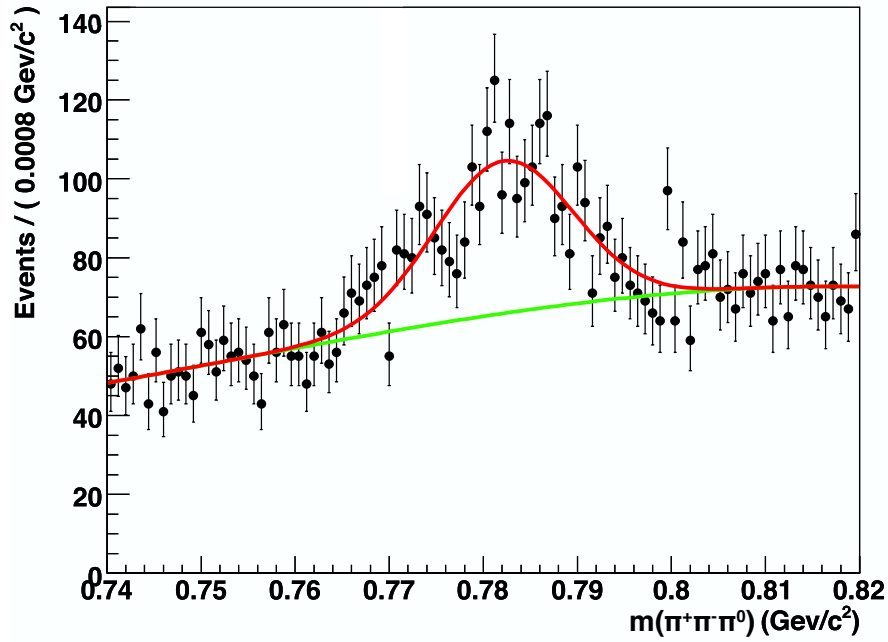


FIG. 3. The $m(\pi^+\pi^-\pi^0)$ invariant mass distribution after signal selections in ΔE and M_{bc} . The displayed fit is used to determine ω candidate selection as described in the text.

TABLE II. Summary of Signal Selections with K_s^0 Veto

Signal Selections
$m(\pi^+\pi^-) \leq 0.48902 \text{ GeV}/c^2$ or $m(\pi^+\pi^-) \geq 0.50672 \text{ GeV}/c^2$
$0.76010 \text{ GeV}/c^2 \leq m(\pi^+\pi^-\pi^0) \leq 0.80474 \text{ GeV}/c^2$
$-0.03551 \text{ GeV} \leq \Delta E \leq 0.03145 \text{ GeV}$
$1.857738 \text{ GeV}/c^2 \leq M_{bc} \leq 1.871802 \text{ GeV}/c^2$

When we float the data widths in the K_s^0 veto analysis, we find 637 ± 89 and 521 ± 85 for the M_{bc} and ΔE signal yields, respectively. These values greatly differ from those with fixed widths, and indeed greatly from each other. We will use the difference between fixed and floating M_{bc} yields as a systematic uncertainty.

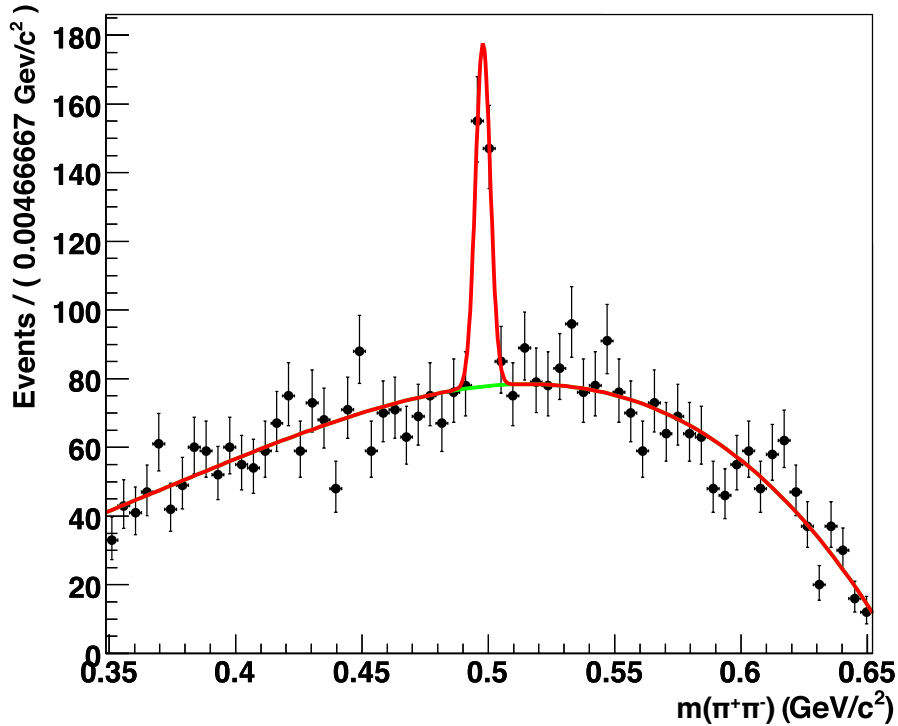


FIG. 4. The $m(\pi^+\pi^-)$ distribution and fit described in text for the $\omega(782)$ candidates as described in the text.

TABLE III. Signal Yields from Fittings Accounting for K_s^0 Effects

	Type	Signal Yield	Signal Efficiency	Yield/Efficiency
K_s^0 Events Subtracted	M_{bc}	667 ± 67	$(17.49 \pm 0.22)\%$	3819
	ΔE	677 ± 72	$(17.06 \pm 0.22)\%$	3969
K_s^0 Veto	M_{bc}	596 ± 62	$(16.13 \pm 0.21)\%$	3694
	ΔE	597 ± 67	$(15.79 \pm 0.21)\%$	3780

We calculate the Branching Fraction using

$$\mathcal{BF} = \frac{N_{D^0 \rightarrow \omega \eta}}{2\epsilon_{D^0 \rightarrow \omega \eta} N_{D^0 \bar{D}^0} \mathcal{BF}_{\omega \rightarrow \pi^+ \pi^- \pi^0} \mathcal{BF}_{\eta \rightarrow \gamma \gamma} \mathcal{BF}_{\pi^0 \rightarrow \gamma \gamma}} \quad (2)$$

where $N_{D^0 \rightarrow \omega \eta}$ is the observed yield and $N_{D^0 \bar{D}^0}$ is the total number of D^0/\bar{D}^0 events. We calculate $N_{D^0 \bar{D}^0}$ by multiplying $\sigma(e^+e^- \rightarrow D^0 \bar{D}^0)$ previously reported by CLEO[4] and our

integrated luminosity. Table IV contains the Branching Fraction inputs.

Comparing the Yield/Efficiency results in Table III we see the K_s^0 Subtraction and Veto are both acceptable methods to deal with K_s^0 contamination giving consistent results. The four efficiency corrected yields have a standard deviation of 115, which is 3.0% of the average efficiency corrected yield of 3816. The efficiency corrected yields are larger in the subtraction method and this method has a conceptual problem. Our subtraction choice is a best guess; there is no clear way to determine how many K_s^0 actually contribute to the signal rather than the background.

We therefore take the M_{bc} yield from the K_s^0 veto analysis as the best measurement. Comparing using M_{bc} and ΔE to extract the yield, we have a fortunately small ± 1 systematic uncertainty from the difference in signal yield and $\pm 0.34\%$ uncertainty from the difference in Efficiency. These give a 2.13% relative uncertainty on the efficiency corrected yield. We also have ± 41 systematic on the yield due to the difference between using fixed and floating widths in M_{bc} fits. These two yield uncertainties give us a total systematic uncertainty on the yield. We find $\mathcal{BF}_{D^0 \rightarrow \omega \eta} = (1.78 \pm 0.19 \pm 0.14) \times 10^{-3}$. The statistical uncertainty comes from the statistical uncertainty in the signal yield. All of the uncertainties are summarized in Table V. The contribution from $\mathcal{BF}(\pi^0 \rightarrow \gamma\gamma)$ is negligible.

TABLE IV. Summary of Branching Fraction Inputs. Branching Fractions are PDG[5] values. Uncertainties are statistical and systematic, respectively.

Quantity	Value
Signal Yield	$596 \pm 62 \pm 1$
Efficiency	$(16.13 \pm 0.208 \pm 0.34)\%$
$\mathcal{BF}(\omega(782) \rightarrow \pi^+\pi^-\pi^0)$	$(89.2 \pm 0.7)\%$
$\mathcal{BF}(\eta \rightarrow \gamma\gamma)$	$(39.31 \pm 0.2)\%$
$\mathcal{BF}(\pi^0 \rightarrow \gamma\gamma)$	$(98.823 \pm 0.034)\%$
$\sigma(e^+e^- \rightarrow D^0\bar{D}^0)$	$(3.66 \pm 0.03 \pm 0.06)nb$
Luminosity	$818 \pm 8pb^{-1}$
$N_{D^0\bar{D}^0}$	2993880

TABLE V. Summary of the uncertainties on $\mathcal{BF}_{D^0 \rightarrow \omega\eta}$.

Source	Value ($\times 10^{-3}$)
Statistical on Yield	± 0.19
Signal Yield	± 0.125
MC Efficiency	± 0.038
Luminosity	± 0.0178
Cross Section	± 0.0326
$\mathcal{BF}(\omega(782) \rightarrow \pi^+\pi^-\pi^0)$	± 0.0140
$\mathcal{BF}(\eta \rightarrow \gamma\gamma)$	± 0.00906
Total Systematic	± 0.137
Total Uncertainty	± 0.23

In summary, in the CLEO-c data we have observed $D^0 \rightarrow \omega\eta$ and measure the average of $D^0 \rightarrow \omega\eta$ and $\bar{D}^0 \rightarrow \omega\eta$ as

$$\mathcal{BF}(D^0 \rightarrow \omega\eta) = (1.78 \pm 0.19 \pm 0.14) \times 10^{-3}. \quad (3)$$

This agrees with the previous observation by BESIII. Our measured branching fraction is roughly a factor of two smaller than predicted. We note that this D^0 decay mode is a CP-eigenstate making it a potentially valuable tool in heavy flavor analysis.

This investigation was done using CLEO data, and as members of the former CLEO Collaboration we thank it for this privilege. This research was supported by the U.S. National Science Foundation.

-
- [1] M. Ablikim *et al.* (BESIII Collaboration), Phys. Rev. D **97**, 052005 (2018).
[2] B. Bhattacharya and J. L. Rosner, Phys. Rev. D, **82** 037502 (2010).
[3] Y. Kubota *et al.* (CLEO Collaboration), Nucl. Instrum. Methods Phys. Res., Sect. A **320**, 66 (1992); D. Peterson *et al.*, Nucl. Instrum. Methods Phys. Res., Sect. A **478**, 142 (2002); M. Artuso *et al.*, Nucl. Instrum. Methods Phys. Res., Sect. A **554**, 147 (2005); CLEO-c/CESR-c

Taskforces & CLEO-c Collaboration, Cornell LEPP Report No. CLNS 01/1742 (2001) (unpublished).

[4] G. Bonvicini *et al.* (CLEO Collaboration), Phys. Rev. D **89**, 072002 (2014).

[5] C. Patrignani *et al.* (Particle Data Group), Chin. Phys. C, **40**, 100001 (2016) and 2017 update.